Non-Covalent Aggregation of Discrete Metallo-Supramolecular Helicates into Higher Assemblies by Aromatic Pathways: Structural and Chemical Studies of New Aniline-Based Neutral Metal(II) Dihelicates

Miguel Vázquez,[a][‡] Manuel R. Bermejo,*[b] Maurizio Licchelli,[a] Ana M. González-Noya,[b] Rosa M. Pedrido,[b] Claudio Sangregorio,[c] Lorenzo Sorace,[c] Ana M. García-Deibe,[b] and J. Sanmartín[b]

Keywords: Fluorescence / Helical structures / Pi interactions / Self-assembly / Supramolecular chemistry

Neutral manganese(II), iron(II), cobalt(II), nickel(II), zinc(II) and cadmium(II) complexes with an *N*-tosyl-substituted N_4-donor Schiff base containing a 4,4′-methylenedianiline residue as spacer [H_2L^a: *N*,*N*′-bis(2-tosylaminobenzylidene)-4,4′-methylenedianiline], and the zinc(II) complex with an analogous ligand [H_2L^b: *N*,*N*′-bis(2-tosylaminobenzylidene)-4,4′-oxodianiline] have been prepared by an electrochemical procedure. FAB and ESI mass spectra of the complexes show peaks due to species corresponding to a general formula $[M_2(L^{a,b})_2 + H]^+$, thereby suggesting their dinuclear nature. A detailed study of the crystal packing in the unit cell of the zinc(II) complex with H_2L^a shows that the helicates aggregate to form discrete prismatic moieties containing three molecules held together by π–π and σ–π interactions. Moreover, the Zn^{II} neutral dihelicate with H_2L^b forms a 3D network in the solid state due to intermolecular π-stacking interactions. ^1H NMR studies of the diamagnetic compounds reported herein have been performed. Finally, the ligand H_2L^a and its Zn^{II} and Cd^{II} complexes have been studied by spectrophotometric and spectrofluorimetric techniques in order to get a better understanding of the formation mechanisms of the complexes and of the nature of their fluorescence emission. Emission studies show that the Zn^{II} and Cd^{II} dihelicates with H_2L^a display a green fluorescence in acetonitrile solution (λ = 473 nm, Φ = 0.03 and λ = 476 nm, Φ = 0.01, respectively).

Introduction

Metallo-helicates are a dynamic research field in supramolecular chemistry.[1–3] However, predicting the result of a self-assembly process is still not easy as it depends on numerous factors, such as the coordination and stereochemical preferences of the metal centres, the structure of the ligand strands or the existence of weak inter- or intramolecular non-covalent connections, such as hydrogen bonds[4] or interactions between aromatic groups.[5]

Aromatic interactions are a very important class of non-covalent intermolecular forces in biology, chemistry and materials science.[6] It has been demonstrated that, in the absence of strong hydrogen-bond donors and acceptors, aromatic groups tend to aggregate via π–π interactions, σ–π (C–H···π) connections, or both, and this trend is magnified when the aromatic groups are electron-poor ring systems.[7] These weak non-covalent bonds can sustain supramolecular architectures,[8] such as the vertical base–base interaction in DNA,[9] the tertiary and quaternary structures of peptides and proteins,[11] the packing of aromatic molecules in crystals,[10] or supramolecular host–guest bonding.[12] Furthermore, Hannon et al. have recently illustrated how metal–ligand and π–π interactions can be used in concert to force the aggregation of helicates into larger nanoscale arrays, such as chiral balls[13] or metallo-supramolecular cylinders.[14] The synthetic method employed to build these assemblies, the so-called "second supramolecular event approach", consists of using an initial supramolecular event to construct small supramolecular units, which are then used as building blocks in a second supramolecular event to give a higher order aggregate.

We have recently embarked upon a program to exploit the helical structural motif as a means of producing larger supramolecular architectures through non-covalent aggregation. In a first approach, we have reported how the introduction of an OH group into an alkyl spacer can provoke the aggregation of neighbouring fluorescent helicates through hydrogen bonding.[15] After that, we decided to ex-

[‡] Present adress: Departamento de Química Inorgánica, Facultade de Química, Universidade de Vigo, 36310 Vigo, Spain
E-mail: miguel.vazquez@uvigo.es
[a] Laboratorio di Chimica Supramolecolare, Dipartimento di Chimica Generale, Università di Pavia, 27100 Pavia, Italy
[b] Departamento de Química Inorgánica, Facultade de Química, Universidade de Santiago de Compostela, 15782 Santiago de Compostela, Spain
E-mail: qimb45@usc.es
[c] UdR INSTM and Dipartimento di Chimica, Università di Firenze, 50019 Sesto Fiorentino (Fi), Italy

plore new routes to employ other non-covalent interactions in the aggregation processes. For this reason we have designed the Schiff-base ligand H_2L^a (Scheme 1), which contains four aniline groups that are potentially electron-deficient ring moieties when coordinating to a metal centre, with the hope that they should induce the aggregation of neighbouring helicate units through aromatic interactions.[16] H_2L^a is also equipped with a long and flexible spacer unit that effectively drives the self-assembly of dihelicates.[17] We have succeeded in synthesising the dinuclear complex of Cu^{II} of this ligand,[18] and herein we describe the synthesis, structural characterisation and absorption, emission and magnetic properties of the manganese(II), iron(II), cobalt(II), nickel(II), zinc(II) and cadmium(II) derivatives of this ligand. Moreover, in order to shed more light on the impact that a change in the flexibility of the spacer could have on the aggregation properties of these complexes, the zinc(II) derivative with an analogous ligand H_2L^b (Scheme 1) has been synthesised and structurally characterised.

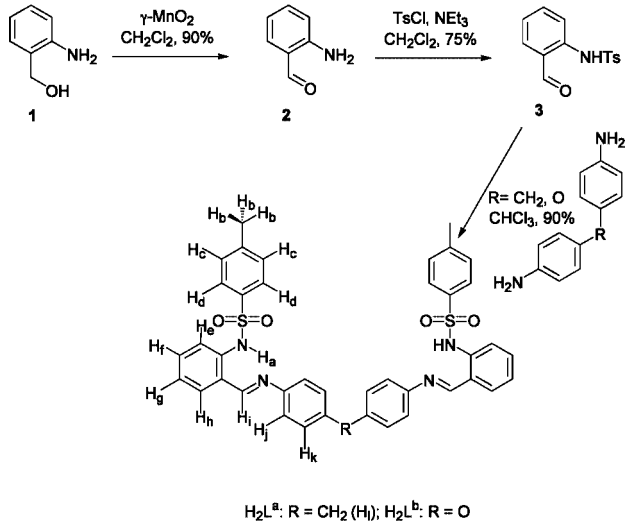

Scheme 1. Synthesis of the ligands H_2L^a and H_2L^b.

Results and Discussion

Synthesis of *N*,*N*′-Bis(2-tosylaminobenzylidene)-4,4′-methylenedianiline (H_2L^a) and *N*,*N*′-Bis(2-tosylaminobenzylidene)-4,4′-oxodianiline (H_2L^b)

Ligands H_2L^a and H_2L^b were synthesised with an overall yield of 60% according to a three-step procedure (Scheme 1).[19] The first step involves the oxidation of 2-aminobenzyl alcohol (**1**) with γ-MnO_2 in dry dichloromethane for 24 h at room temperature, under argon to give 2-aminobenzaldehyde (**2**).[20] Subsequently, the *N*-tosylation of **2** with tosyl chloride and triethylamine to give 2-tosylaminobenzaldehyde (**3**) was performed. Compound **3** has also been prepared and structurally characterised by us by another method.[21] Finally, Schiff-base condensation of **3** and 4,4′-methylenedianiline or 4,4′-oxodianiline in chloroform at reflux temperature afforded ligands H_2L^a and H_2L^b, respectively. These ligands were satisfactorily characterised (see Exp. Sect.).

Electrochemical Synthesis of the Complexes

A series of metal neutral complexes was obtained by electrochemical oxidation[22] of the corresponding metal anode in an acetonitrile solution of the corresponding ligand in the presence of a small quantity of tetraethylammonium perchlorate as supporting electrolyte. The electrochemical efficiencies of the cells were close to 0.5 mol F^{-1}, which are compatible with the following reaction scheme:

Cathode: $2\ H_2L^{a,b} + 4e^- \rightarrow 2\ H_2\ (g) + 2\ (L^{a,b})^{2-}$

Anode: $2\ (L^{a,b})^{2-} + 2M \rightarrow [M(L^{a,b})]_2 + 4\ e^-$

This synthetic procedure allowed us to obtain neutral metal complexes of the type $[M(L^{a,b})]_2{\cdot}(CH_3CN)_n$ (n = 0–2) with high purity and in very good yield. The empirical formulae found, namely $[M(L^a)]{\cdot}(CH_3CN)_n$ (M = Mn, Fe, Co, Ni, Zn, Cd; n = 0–2) and $[Zn(L^b)]{\cdot}(H_2O)_4$, suggest that the metals react with the ligands in a 1:1 molar ratio. All of them seem to be stable in the solid state and, with the exception of the manganese(II) and iron(II) complexes with H_2L^a, also in solution. They are fairly soluble in the most common polar aprotic organic solvents, but totally insoluble in both apolar or protic media.

The complexes with H_2L^a show a shift of the ν(C=N) absorption to lower wavenumbers (7–25 cm^{-1}; cf. 1621 cm^{-1} in the free ligand). In addition, a shift of the ν(C–N) absorption to lower wavenumbers is also observed (34–48 cm^{-1}; cf. 1337 cm^{-1} in the free ligand). Moreover, the zinc(II) complex with H_2L^b shows a slight shift of 7 cm^{-1} for ν(C=N) (1617 cm^{-1} in the free ligand) and a shift of 40 cm^{-1} for ν(C–N) (1340 cm^{-1} in the free ligand), both to lower wavenumbers. These IR data suggest that both imine and amide nitrogen atoms are involved in coordination to the metal centres in all the complexes.

The FAB mass spectra of the complexes show peaks due to fragments $[M_2(L^{a,b})_2 + H]^+$. Such results imply a successful coordination of the ligands to the metals and suggest the dinuclear nature of the complexes. Fragments containing solvent molecules were not observed, which points to the solvate nature rather than to a coordination behaviour of the solvent molecules. Higher molecular weight peaks, which could suggest the presence of supramolecular aggregates, were not observed in any spectra. In order to assess the identity of the complex species formed in solution by the ligands H_2L^a and H_2L^b more clearly, further investigations were performed by electrospray ionisation mass spectroscopy (ESI-MS). All the spectra exhibit base peaks (ca. 100%) corresponding to $[M_2(L^{a,b})_2 + H]^+$ fragments. These data suggest that the [2+2] complexes are the main species in solution.

Crystal Structure of $[Zn(L^a)]_2 \cdot CH_3CN$ (5)

Recrystallisation of **5** from acetonitrile by slow concentration afforded yellow crystals for which we determined the molecular structure by X-ray crystallography.[23]

The asymmetric unit of the zinc(II) dihelicate **5** (Figure 1) contains two Zn atoms, two ligands and one acetonitrile molecule. The Zn–Zn distance is 11.83 Å and the ligands wrap around the two zinc centres to form a double helix with helical twists of 140.0° ([Zn1–N3–N2–Zn2) and 143.5° (Zn1–N7–N6–Zn2). The distortion from an ideal tetrahedral geometry is shown by the angles between the nitrogen and zinc atoms, which range from 93.0° to 126.8° for Zn1, and from 93.6° to 126.9° for Zn2.

Each ligand forms two six-membered chelate rings, which are nearly planar, one around each zinc atom. The angle between these chelate rings at both metal centres are 96.03(1)° for Zn1 and 103.94(1)° for Zn2. Two oxygen atoms from the tosyl groups interact weakly with each metal centre (Zn–O distances range from 2.65 to 2.87 Å). All other bond lengths are similar to those found in other tetrahedral zinc(II) complexes with related Schiff-base ligands.[15,19,24] The phenyl rings of the diarylmethane spacer are face-to-face π-stacked with those on the adjacent ligand strand [centroid–centroid distances: rings C22 to C27 and C63 to C68 = 4.19 Å; rings C15 to C20 and C55 to C60 = 4.01 Å; angles between ring planes: rings C22 to C27 and C63 to C68 = 27.11(2)°, rings C15 to C20 and C55 to C60 = 18.02(2)°]. All these distances and angles reveal the non-equivalence of the environment of the two zinc atoms and of both ligand units, which gives rise to a certain degree of asymmetry.[5a,19] This coordinative asymmetry leads to the formation of two grooves of different size in the main body of the metallo-organic double helix, reminiscent of the structure of DNA.[25] A good approximation to the wrapping angle of the helicate could be the torsion angle formed by the two metal ions, that define the helical axis of the helicate, and the outer donor atoms of the same ligand strand that coordinate these two metal centres. In our case these torsion angles are 279.5° for N8–Zn1–Z2–N5 and 280.4° for N4–Zn1–Zn2–N1.

A great number of intermolecular face-to-face and edge-to-face aromatic interactions between neighbouring helicates are present in the crystal cell. A detailed study of the

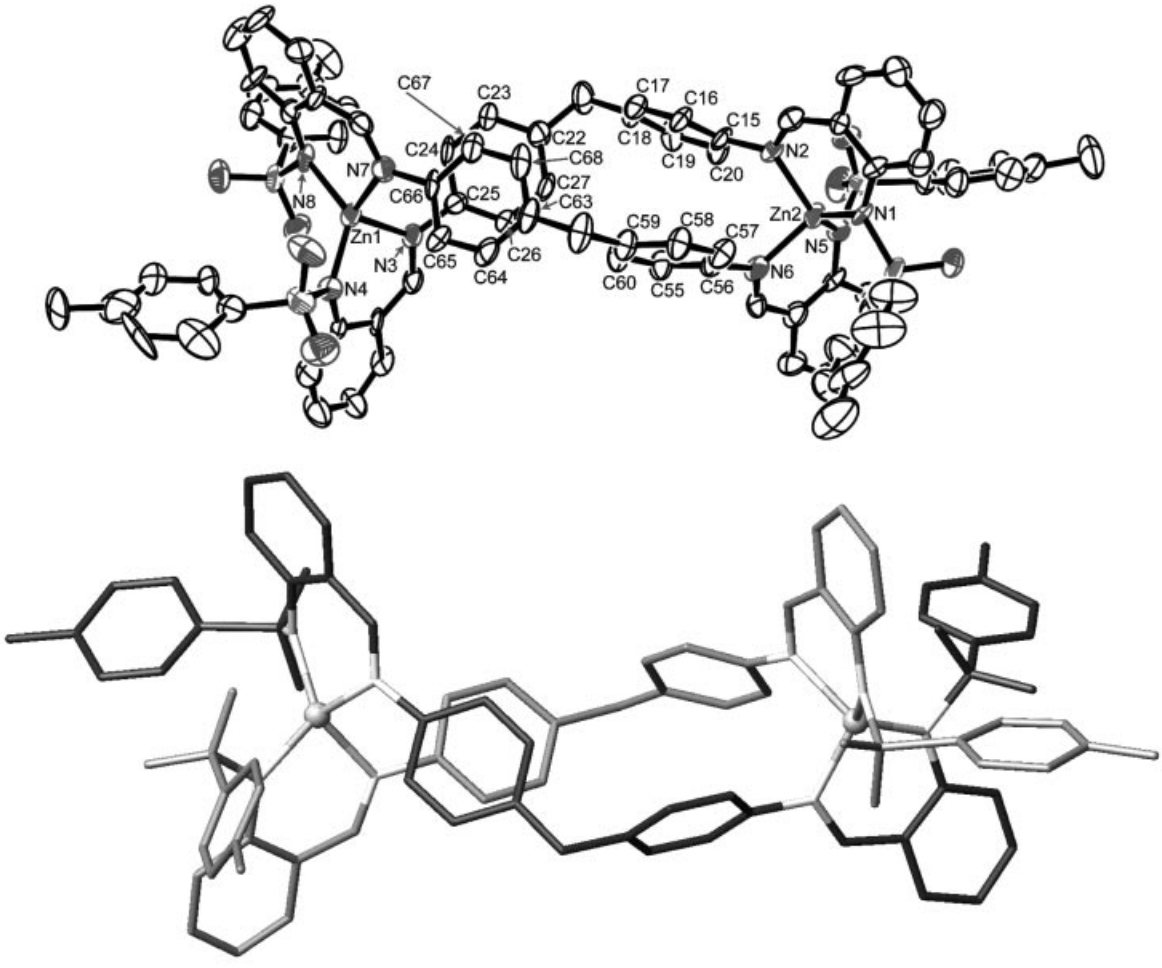

Figure 1. Top: ORTEP representation of the molecular structure of $[Zn(L^a)]_2 \cdot CH_3CN$ (**5**). Thermal ellipsoids are shown at the 40% probability level. Bottom: Stick representation of the X-ray crystal structure of **5**. Hydrogen atoms and the solvent molecule have been omitted for clarity.

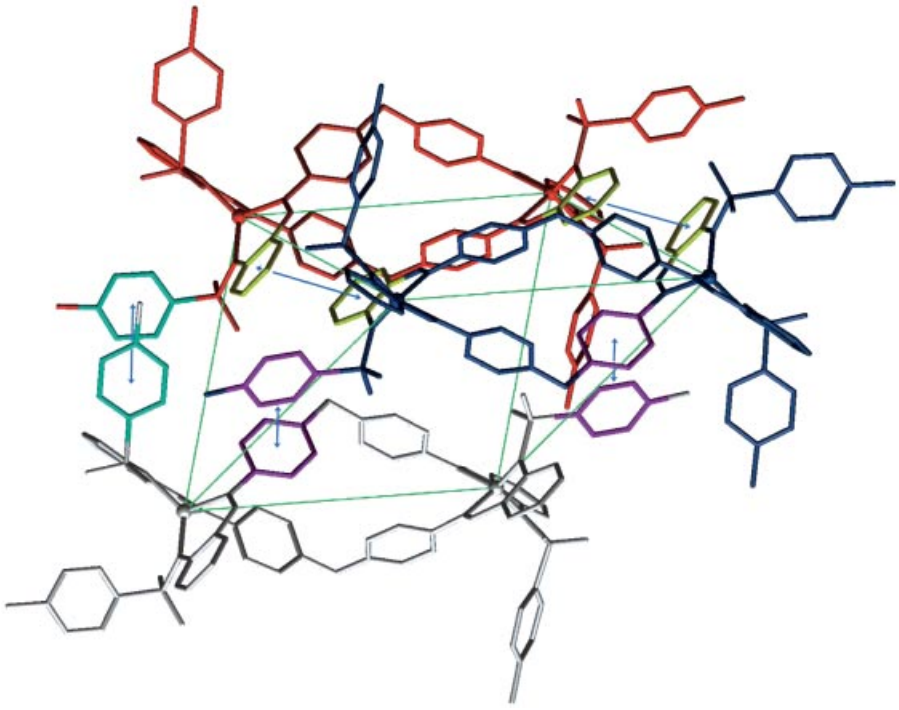

Figure 2. Part of the unit cell of **5** exhibiting the three different types of intermolecular aromatic interactions (cyan, yellow and pink) between three adjacent dihelicates (blue, grey and red). The dinuclear helicates aggregate to form discrete supramolecular prismatic assemblies of three molecules.

crystal packing reveals that the Zn^{II} dihelicates aggregate to form discrete prismatic moieties of three metallo-supramolecular members held together by π–π and σ–π connections.

There are three aromatic supramolecular interactions of different nature in each "triangular prism"; they are coloured cyan, yellow and pink in Figure 2. Both the yellow and cyan interactions are offset π–π interactions, while the pink ones are σ–π. The red dihelicate is connected to the blue one through two identical offset π–π interactions (yellow) between the aromatic rings of their benzylidene binding moieties ($centroid_{red}$–$centroid_{blue}$ distance = 3.89 Å). Moreover, the red dihelicate is connected to the grey one through a unique offset π–π interaction (cyan) between the aromatic rings of their terminal tosyl groups ($centroid_{red}$–$centroid_{white}$ distance = 4.07 Å). Finally, the white dihelicate is connected to the blue one through two identical edge-to-face interactions (pink) using one aromatic ring from the spacer and another from the terminal tosyl group, in a double contact (H_{blue}–$centroid_{white}$ distance = 3.18 Å). These distances are similar to those reported in the literature by us[18] and others[26] for analogous helicates, but shorter than that found for $[Zn(L^b)]_2$ (see below).

Figure 3 shows two different views of two adjacent triangular prisms, painted red and green. There are no π–π or σ–π aromatic interactions between neighbouring prismatic aggregates − they are discrete moieties. Each prism contains both types of helical enantiomer (left-handed and right-handed). The red prism (Figure 3b, left) contains one left-handed and two right-handed helicates, while the green prism (Figure 3b, right) contains one right-handed and two left-handed helicates. The unit cell encloses both isomers in 50% yield.

In summary, the discrete dinuclear dihelicates aggregate in the solid state into groups of three molecules that form an unprecedented assembly of six Zn^{II} ions and six ligands. The volume of the triangular prism defined by the six Zn^{II} ions is 598 $Å^3$ (Figure 4).

Crystal Structure of $[Zn(L^b)]_2 \cdot CH_3CN$

Yellow crystals of $[Zn(L^b)]_2 \cdot CH_3CN$ suitable for X-ray studies[27] were obtained by slow concentration of a saturated acetonitrile solution of $[Zn(L^b)]_2 \cdot (H_2O)_4$ (**7**). The structure of this complex (Figure 5) reveals the formation of a binuclear zinc(II) complex, with the ligands spanning both metal centres and intertwined to give a perfectly symmetrical double helix (symmetry space group of the unit cell = *Fddd*). A racemic mixture of both enantiomers (left- and right-handed) is observed in the crystal cell.

Each zinc(II) centre occupies a four-coordinate distorted tetrahedral environment, being bound by two aminobenzylidenimine units, one from each ligand. Thus, both ligands act as bisbidentate N_4 donors. The distortion from an ideal tetrahedral geometry is shown by the angles between the nitrogen and zinc atoms, which range from 92.2° to 128.0°. Each ligand forms two six-membered chelate rings, which are nearly planar, one around each metal atom. The angle between the chelate rings in both metal centres is 112.9°. Two oxygen atoms from the tosyl groups interact

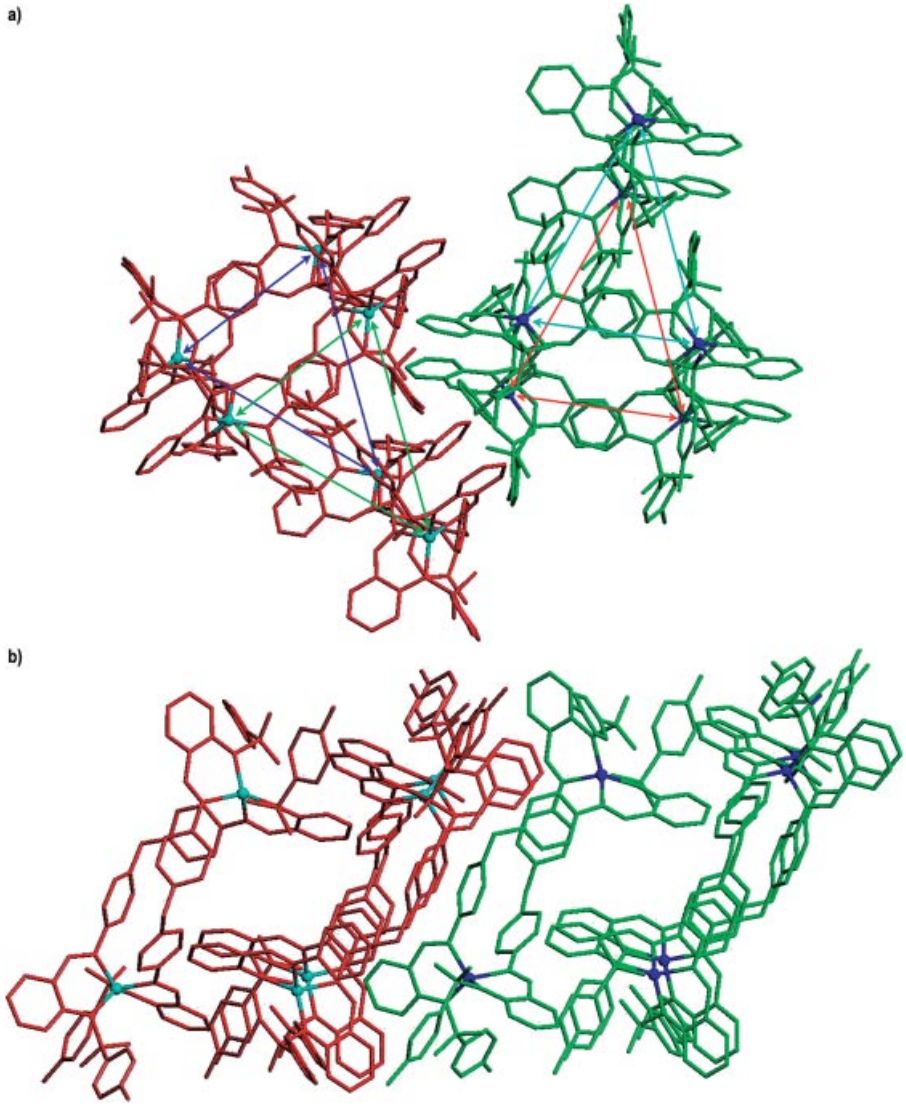

Figure 3. Two different views of two neighbouring prisms (red and green) in the unit cell of **5**. There are no aromatic interactions (π–π or σ–π) between adjacent prismatic aggregates.

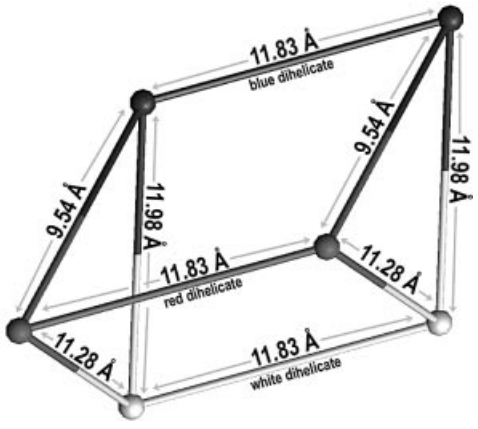

Figure 4. Schematic representation of the supramolecular triangular prism of zinc(II) dihelicates in **5** showing the inter- and intramolecular Zn–Zn distances. The spheres represent the zinc(II) ions, and their colour indicates their original dihelicate, as shown in Figure 2. The volume of the geometrical solid defined by the six Zn^{II} ions is 598 $Å^3$.

weakly with each metal centre (Zn–O distance = 2.69 Å). All the other bond lengths are similar to those found in other tetrahedral zinc(II) complexes with similar N_4 Schiff bases.[15,19,24]

The phenyl rings of the oxodianiline spacer are face-to-face π-stacked with those on the adjacent ligand strand (centroid–centroid distance = 3.99 Å; angle between ring planes = 12.9°). To achieve this, the two ligand units are pulled symmetrically along the helical axis. The helical twist of the ligand strands around the helical axis, defined by the N(1)–Zn(1)–Zn(1_3)–N(1_4) dihedral angle, is 268.8°.

The intermolecular π-stacking interactions present in this crystal structure, which are responsible for the aggregation of the discrete zinc(II) helicate units into a polymeric 3D network of helicates, are very similar to those described in our previous communication.[18] Each Zn^{II} dihelicate uses two aromatic rings to connect to another helical unit, one from the oxodianiline spacer and the other from the benzylidene binding moiety, in a double interaction. Overall, each

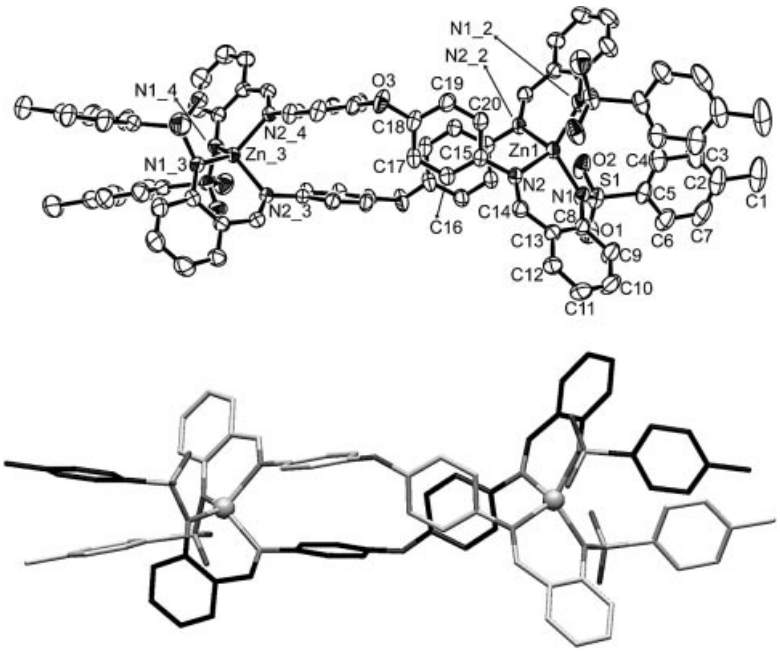

Figure 5. Top: ORTEP representation of the molecular structure of $[Zn(L^b)]_2{\cdot}CH_3CN$ Thermal ellipsoids are shown at the 50% probability level. Bottom: Stick representation of the X-ray crystal structure of $[Zn(L^b)]_2{\cdot}CH_3CN$. Hydrogen atoms and the solvent molecule have been omitted for clarity.

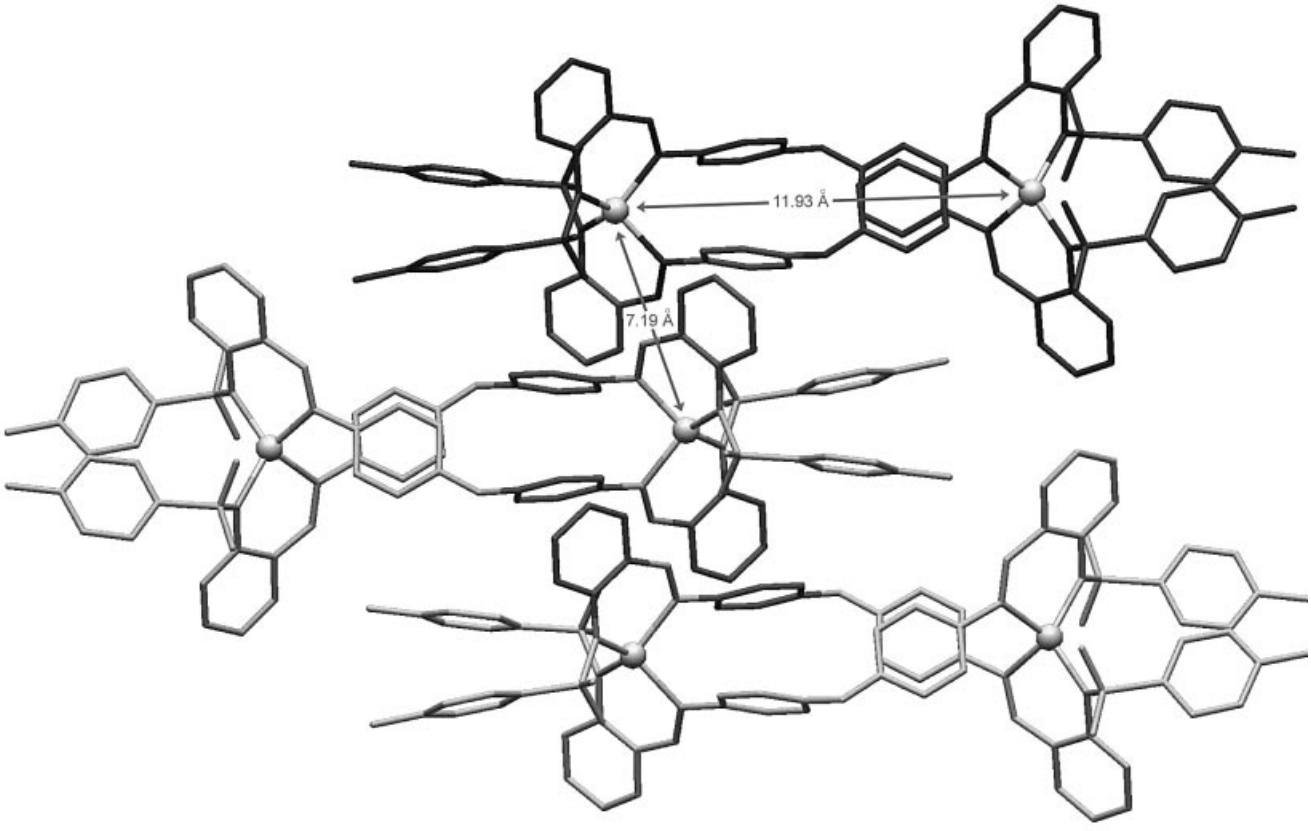

Figure 6. A representation of part of the unit cell of $[Zn(L^b)]_2{\cdot}CH_3CN$, showing the double π-stacking connections established between adjacent dihelicates. This is a 2D view of the crystal cell; π–π connections on the left side of the central dihelicate that grow normal to the plane of the paper must be considered equivalent. Interestingly, the intermolecular Zn–Zn distance (7.19 Å) is shorter than the intramolecular one (11.93 Å).

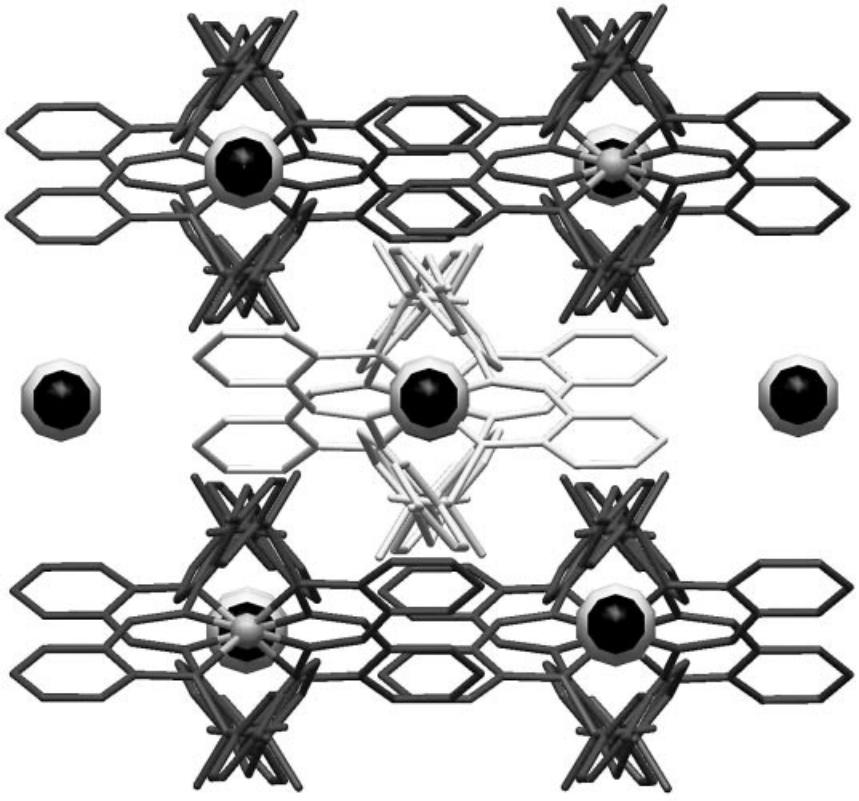

Figure 7. A perspective of the unit cell of $[Zn(L^b)]_2 \cdot CH_3CN$. It can be considered as a 3D supramolecular solid into which acetonitrile guest molecules (white-black spheres) are absorbed.

helicate is connected to another four molecules, through eight identical offset π–π interactions, forming a 3D network of helicates (Figure 6). The distance between the centroids of the intermolecular stacked aromatic rings is 4.80 Å. The "displacement angle" between these stacked rings, defined as the angle between the centroids vector and the normal to the benzylidene ring plane, is 21.7°. Moreover, the distance between the two closest zinc(II) centres of connected dihelicates is shorter (7.19 Å) than the intramolecular Zn–Zn distance (11.93 Å).

Another interesting structural feature of this complex is the presence of two, totally unbound acetonitrile molecules per formula unit that fill the 3D body of the network (Figure 7). This fact shows the capability of the array to include a large number of small, neutral guest molecules.[28] It must be noted that while a number of open frameworks have been assembled by the reactions of metal ions with a large variety of organic molecules, such as di-, tri-, and polytopic N-bound organic linkers or carboxylate linkers (i.e. 4,4-bipyridine[29] and benzene-1,3,5-tricarboxylate[30]), those sustained by π–π interactions are still rare or lacking.[31] Moreover, the use of helical metal-organic architectures as building blocks for the formation of 3D networks has been explored only recently.[26]

This supramolecular situation is quite different to that described above for the other Zn^{II} helicate **5**, where the π–π and σ–π interactions between the aromatic rings of different complexes allow the formation of discrete prismatic aggregates of three helicates. However, it is very similar to that found for the recently reported Cu^{II} derivative with H_2L^a,[18] the difference being that the metal centres in the copper(II) dihelicate occupy very distorted (near square-planar) tetrahedral environments.

The ligand H_2L^b is more rigid than H_2L^a due to the substitution of the CH_2 group in the spacer by an oxygen atom. In addition, the Zn^{II} ion is coordinatively more flexible than Cu^{II}. Taking all this into account, we reasoned that the introduction of more rigidity into any of the building blocks that form a helicate (the ligands or the metal centres) leads to the formation of more-symmetric dihelicates. Moreover, this high symmetry seems to support the self-aggregation of the helicates into polymeric arrays rather than discrete assemblies. Therefore, we suggest that more-rigid building blocks facilitate the self-aggregation of the dihelicates into 3D frameworks.

Magnetic Studies

The occurrence of a coupling between metal centres reported for the Cu^{II} derivative of the ligand H_2L^a[18] could not be confirmed by measurements on the other paramagnetic complexes. The magnetic moments of all the paramagnetic complexes reported herein were recorded in the solid state between 2 and 300 K. The values of the magnetic moments, obtained by the Curie–Weiss fit of susceptibility

data, are in the range expected for magnetically diluted tetrahedral metal(II) ions.[32] The temperature dependence of the magnetic susceptibilities for all the complexes shows deviation from Curie behaviour at low temperature ($T < 30$ K).

The occurrence of a coupling between metal centres could not be confirmed by measurements of the magnetic susceptibilities on these paramagnetic complexes. Indeed, even if present, the coupling is so weak that its presence would be masked in all the other complexes by zero-field splitting effects, whose energies are comparable to, or even larger in magnitude than, those involved in exchange-coupling. In particular, it should be noted that the electronic ground state in tetrahedral coordination for Ni^{II} ($^3T_1$) and Fe^{II} ($^5T_2$) is orbitally degenerate (although this degeneracy can be removed by low-symmetry effects) and that the magnetic behaviour of tetrahedral Co^{II} is largely affected by spin-orbit coupling of the low-lying excited $^4T_2$ state and the ground $^4A_1$ one. In this framework the observed deviation from Curie–Weiss behaviour observed at low temperature for these systems should be more likely attributed to single-ion effects than to exchange interactions.[33]

NMR Studies

All the NMR experiments carried out with the ligand H_2L^a and the Zn^{II} and Cd^{II} complexes **5** and **6** were recorded with $CDCl_3$ as solvent. The NMR studies with the ligand H_2L^b and the Zn^{II} complex **7** were recorded in [D_6]-DMSO. Assignment of the signals was based on previous results[15,19,24] and on the available literature.[17,34] A comparison between the spectra of the free ligand and those of their respective complexes highlights some interesting features. The NH protons (H_a in Scheme 1) present in the free ligands disappear in the spectra of the complexes, in agreement with the deprotonation of the sulfonamide groups, and the imine hydrogen atoms (H_i) show a shift to higher field for the three complexes (ca. 0.15 ppm), thus demonstrating the coordination of the imine groups to the metal centre. Moreover, the imine protons of the cadmium complex **6** are flanked by satellites arising from spin-spin coupling to $^{111/113}Cd$, suggesting that the complex is kinetically inert on the NMR timescale. The FAB and ESI mass spectra of **5** and **6** suggest the existence of dinuclear $[M(L^a) + H]_2$ species in solution. In addition, their room temperature ^1H NMR spectra in chloroform reveal single sharp sets of proton resonances, indicating the existence of just one species in solution for both complexes. The non-diastereotopic CH_2 protons of the spacer (H_l) of the ligand H_2L^a permitted us to identify their nature. In a dihelical structure, these two protons will be equivalent and a singlet must therefore be observed: in both spectra, a single set of resonance signals are detected, and there is no evidence of the pair of doublets which is characteristic of the CH_2 group in the non-helical box architecture. Thus, the NMR spectroscopic data lead us to conclude that these solution species must also be neutral dimeric helicates of $[M(L^a)]_2$ stoichiometry. The substitution of the non-diastereotopic CH_2 protons by an oxygen in H_2L^b makes it impossible to prove whether the dihelical nature of the [2+2] species of **7** is present in solution.

UV/Vis Absorption and Fluorescence Emission Studies

Absorption and fluorescence data recorded for the ligand and its metal complexes are reported in Table 1. The UV/Vis absorption spectrum of H_2L^a, in acetonitrile solution, exhibits three strong bands (244, 328 and 342 nm). Coordination to M^{II} ions leads to a substantial variation of the absorption spectra. In particular, a new band appears with a maximum in the 370–390 nm range. Unfortunately, all attempts to record the UV/Vis absorption spectra of the manganese(II) and iron(II) derivatives with H_2L^a were unsuccessful because of their poor stability in solution.

Table 1. Absorption and fluorescence data recorded in CH_3CN.

Compound	λ [nm]	ε [$M^{-1}\,cm^{-1}$]	λ_{em} [nm]	Φ
H_2L[a]	244 328 342	49200 26400 26100	475	$<10^{-3}$
3	244 302 384	84800 47300 28700	–	–
4	246 292 388	154900 63500 41400	–	–
5	246 316 379	110000 52100 40700	473	0.03
6	243 318 371	74700 32500 27600	476	0.01

[a] UV/Vis spectra recorded in DMSO.

Fluorescence emission studies in acetonitrile solution show that H_2L^a has a residual luminescence at about 475 nm ($\Phi < 0.001$). The chelation of metal ions to $(L^a)^{2-}$ induces an enhancement of the fluorescence emission (CHEF effect), which is significantly more pronounced for zinc(II), as indicated by the quantum yields values determined for both complexes in acetonitrile ($\Phi = 0.03$ and 0.01 for Zn^{II} and Cd^{II}, respectively). Complex **5** displays a single exponential fluorescence decay at 473 nm, with a lifetime of $\tau = 1.75 \pm 0.03$ ns. The fluorescence lifetime of **6** could not be measured because it is shorter than the response time of our equipment ($\tau < 1$ ns). Moreover, the excitation spectrum of **5** ($\lambda_{em} = 473$ nm) is coincident with the absorption spectrum. Finally, it must be noted that complex **5** does not exhibit triplet emission at low temperature.

Although the origin of the luminescence[15,19] displayed by these compounds remains unknown we have recently proposed that the fluorescence active unit of similar tosylimine derivatives is located on the 2-tosylaminobenzaldehyde residue, since this exhibits an intense luminescence at

about 498 nm in CH_3CN solution. These new data confirm the important role that the spacer group of this family of tosylimine ligands plays on their fluorescence properties: 4,4′-methylenedianiline, (1*R*,2*R*)-diaminocyclohexane and 1,3-diamino-2-propanol spacers quench the luminescence of the 2-tosylaminobenzaldehyde residue effectively, whereas other spacers such as 1,2-diaminoethane or 1,3-diaminopropane do not prevent the fluorescence emission of their corresponding free ligands.

The relative stability of **5** and **6** was studied by spectrophotometric and spectrofluorimetric experiments. Trifluoroacetic acid (TFA) was added to an acetonitrile solution of these complexes in order to test their behaviour in acidic media. No aqueous solvents were used due to the low solubility of **5** and **6** in these media. For both complexes, the addition of an excess of TFA makes the absorption spectra to become superimposable on that of the free ligand. Such evidence suggests that a demetallation reaction takes place with a protonation of the $(L^a)^{2-}$ species. The titration profiles indicate that the demetallation is complete after addition of about 5 equiv. of TFA for the Zn^{II} complex and about 1 equiv. for the Cd^{II} complex. Therefore, the zinc complex appears to show a higher stability towards acidis. In addition, the formation of only one isosbestic point in the UV/Vis spectra of **5** and **6** during the addition of TFA suggests the existence of only two species in solution: the corresponding complex and the free ligand. Figure 8 shows the variation of the UV/Vis absorption spectra of **5** upon the addition of a standard acetonitrile solution of TFA.

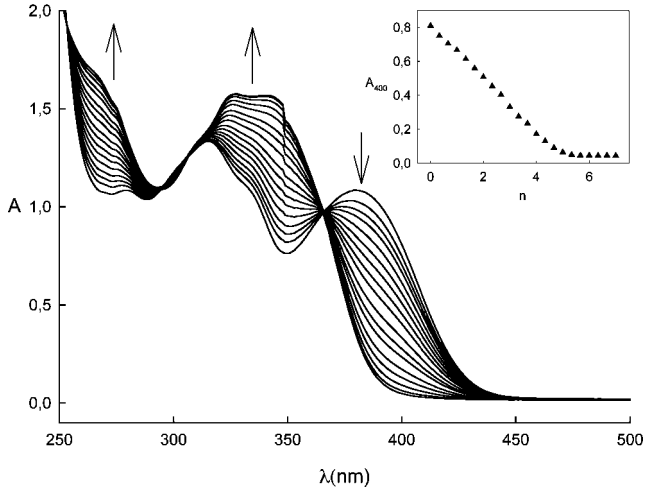

Figure 8. Spectrophotometric titration of an acetonitrile solution of **5** (3×10^{-5} M) with a standard solution of TFA. Inset: absorption intensity at 400 nm (A_{400}) vs. equiv. of TFA (n).

Similar results were obtained by fluorescence measurements. Figure 9 shows the variation of the emission spectra of **5** upon the addition of a standard acetonitrile solution of TFA. The successive addition of acid leads to a progressive decrease of the fluorescence intensity at 473 nm, which, at the end of the titration (after approx. 5 equiv. of TFA), results in a residual emission ($\Phi < 10^{-3}$) characteristic of the free ligand. In the case of the cadmium(II) complex the fluorescence at 476 nm ($\Phi = 0.01$) is completely quenched after the addition of about 1 equiv. of TFA. These data are consistent with the demetallation reaction mentioned above.

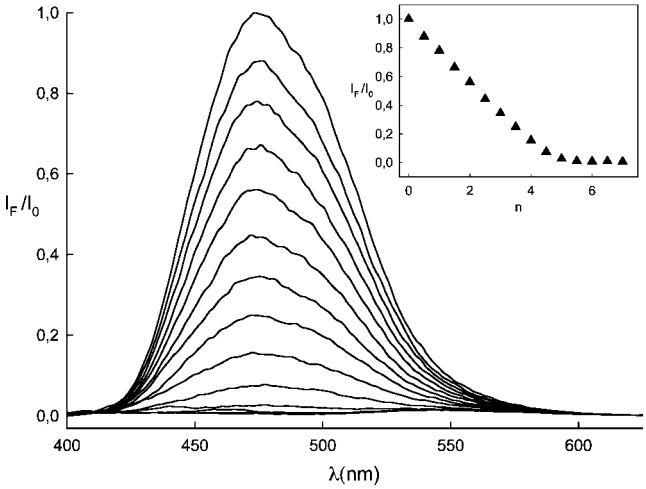

Figure 9. Spectrofluorimetric titration (λ_{exc} = 366 nm) of an acetonitrile solution of **5** (3×10^{-5} M) with a standard solution of TFA. On acid addition, the emission band at 473 nm decreases and the green fluorescence is quenched. Inset: fluorescence intensity at 473 nm (I_F/I_0) vs. equiv. of TFA (n).

Conclusions

In this work we have confirmed the capability of the N_4 Schiff-base ligands *N*,*N*′-bis(2-tosylaminobenzylidene)-4,4′-methylenedianiline (H_2L^a) and *N*,*N*′-bis(2-tosylaminobenzylidene)-4,4′-oxodianiline (H_2L^b) to support the aggregation of discrete helicates into higher supramolecular assemblies through intermolecular non-covalent aromatic interactions. The ligand H_2L^b is more rigid than H_2L^a due to the substitution of the CH_2 group in the spacer by an oxygen atom. The molecular structure of the zinc(II) dihelicate with H_2L^a shows that the discrete complexes aggregate to form discrete prismatic moieties of three molecules held together by π–π and σ–π interactions. The resulting nanoscale structure is a supramolecular assembly of six Zn^{II} ions and six ligands. The volume of the nanoscale triangular prism defined by the six Zn^{II} ions is 598 Å^3. The Zn^{II} complex with H_2L^b forms a polymeric 3D framework in the solid state due to π-stacking interactions between the aniline moieties of discrete dihelicates. Taking into consideration these two structures and those of the previously reported Cu^{II} dihelicate with the ligand H_2L^a,[18] we suggest that an increment of the "rigidity" in any of the building blocks that form this class of neutral dihelicates (aniline ligands and metal centres) definitively favours the self-aggregation of the complexes into 3D polymeric frameworks rather than discrete assemblies.

In addition, the ligand H_2L^a and its diamagnetic Zn^{II} and Cd^{II} complexes have been studied by NMR, spectrophotometric and spectrofluorimetric techniques, leading to

an understanding of their formation mechanism as well as their structure in solution. Fluorescence studies also confirmed the emissive properties of the tosylaminobenzylidene moiety and the important role that the spacer group of this family of tosylimine ligands plays in this sense. The 4,4′-methylenedianiline spacer avoids luminescence of the 2-tosylaminobenzylidene residue, and only the chelation of Zn^{II} to $(L^a)^{2-}$ involves a significant enhancement of the fluorescence emission (λ_{em} = 473 nm, Φ = 0.03). On the other hand, the Cd^{II} dihelicate displays a low green fluorescence in acetonitrile solution (λ = 476 nm, Φ = 0.01). Finally, it must be noted that the Zn^{II} dihelicate displays a single exponential fluorescence decay at 473 nm, with a lifetime, τ, of 1.75 ± 0.03 ns.

We are currently exploring how to integrate further supramolecular interactions to design more-sophisticated assembly pathways based on multiple recognition events.

Experimental Section

Materials: All the starting materials were purchased from Aldrich and used without further purification. All metals were used as plates, except manganese metal, which was used as pellets. All of them were washed with a dilute solution of hydrochloric acid prior to the electrolysis.

Physical Measurements: Elemental analyses were performed with a Carlo Erba EA 1108 analyzer. The infrared spectra were recorded as KBr pellets with a Bio-Rad FTS 175 spectrophotometer in the range 4000–600 cm^{-1}. Fast atom bombardment (FAB) mass spectra were recorded with a Kratos MS-50 mass spectrometer, employing Xe atoms at 70 keV with *m*-nitrobenzyl alcohol as the matrix. ESI spectra were obtained with an LCQDECA ion-trap mass spectrometer equipped with an electrospray ionisation ion source and controlled by Xcalibur software 1.1 (Thermo-Finnigan). Magnetic susceptibilities of paramagnetic complexes were measured between 2 and 300 K with applied magnetic fields of 0.1 and 1 Tesla using a Cryogenic S600 SQUID magnetometer. Given the expected large anisotropy of Fe^{II}, Co^{II} and Ni^{II} derivatives, they were pressed into pellets to avoid the orientation of polycrystalline powders. Data were corrected for the magnetism of the sample holder, which was determined separately in the same temperature range and field, and the underlying diamagnetism of each sample was estimated from Pascal's constants.[35] The NMR spectra were recorded with a Bruker DPX-250 spectrometer, with $CDCl_3$ and $[D_6]$DMSO as solvents. UV/Vis spectra were recorded with a Varian Cary 100 spectrophotometer; emission and excitation spectra were recorded with a Perkin–Elmer LS-50B luminescence spectrometer. Spectrophotometric and spectrofluorimetric titrations were performed on 10-mL samples of solutions of the complexes (3×10^{-5} M) in CH_3CN, by microaddition of CH_3CN stock solutions of TFA. In each experiment, the overall addition was limited to about 200 μL, so that the volume increment was not significant. The fluorescence decay curves were recorded with an Edinburgh Instruments Model FL 900 time-correlated single-proton counting spectrometer, at the Centro Grandi Strumenti (Università di Pavia). The instrument was operated with a flash lamp filled with H_2 at a pressure of 0.4 atm, with a frequency of 40 kHz and a pulse width of 1.0 ns. The relative fluorescence quantum yields were obtained by the optically diluted method,[36] with dansyl amide (Φ = 0.37 in CH_3CN) as reference.[37]

2-Aminobenzaldehyde (2): 2-Aminobenzyl alcohol (1 g, 8.0 mmol) was dissolved in dry dichloromethane (50 mL) and γ-MnO_2 (0.70 g, 8.0 mmol) was added under argon. The reaction mixture was stirred at room temperature for 24 h. After this, the resulting mixture was filtered through a silica gel bed. The filtrate was concentrated under reduced pressure to leave an oily residue. The residue was then passed through a short silica gel column (silica gel, hexane/ethyl acetate, 5:1) to afford the pure aldehyde **2**.[20] Yield: 0.861 g (90%). FAB MS: *m*/*z* = 122.1 [M^+ + H]. C_7H_7NO: calcd. C 69.4, H 5.8, N 11.6; found C 69.3, H 5.9, N 11.6.

2-Tosylaminobenzaldehyde (3): Aldehyde **2** (0.86 g, 7.10 mmol) was dissolved in dry dichloromethane (50 mL) and tosyl chloride (1.36 g, 7.10 mmol) and triethylamine (5.0 mL, 35.5 mmol) were added under argon. The reaction mixture was heated at reflux temperature for 8 h. After this, the resulting mixture was filtered through a thin Celite bed. The solution was then treated with acid water (pH = 4–5, 3 × 100 mL) and the organic solution dried with Na_2SO_4. The solvent and the excess of triethylamine were removed in vacuo and the residue was recrystallised from chloroform.[19,21] Yield: 1.487 g (75%). FAB MS: *m*/*z* = 276.1 [M^+ + H]. $C_{14}H_{13}NO_3S$: calcd. C 61.1, H 4.7, N 5.1, S 11.6; found C 69.3, H 4.6, N 5.1, S 11.7.

***N*,*N*′-Bis(2-tosylaminobenzylidene)-4,4′-methylenedianiline (H_2L^a):** 4,4′-Methylenedianiline (0.50 g, 2.54 mmol) was added to a chloroform solution (150 mL) of **3** (1.40 g, 5.08 mmol). This mixture was heated (70 °C) and the volume of the solution was reduced to about 30 mL over period of 3 h in a Dean–Stark trap. The resulting solution was filtered and then concentrated. The orange powdery solid was collected by filtration, washed with diethyl ether (25 mL), and dried in vacuo. Yield: 1.501 g (80%). FAB MS: *m*/*z* = 713.1 [M^+ + H]. $C_{41}H_{36}N_4O_4S_2$: calcd. C 69.1, H 5.1, N 7.8, S 9.0; found C 69.1, H 5.2, N 7.9, S 8.9. IR (KBr): $\tilde{\nu}$ = 1621 $\nu_{C=N}$, 1337 ν_{C-N}, 1287 ν_{asSO_2}, 1156 ν_{sSO_2} cm^{-1}. ^1H NMR (250 MHz, $CDCl_3$, 25 °C): δ = 12.98 (s, 2 H, H_a), 8.48 (s, 2 H, H_i), 7.73 (d, ^3J = 8.1 Hz, 4 H, H_d), 7.66 (d, ^3J = 7.8 Hz, 2 H, H_e), 7.37–7.15 (m, 16 H, $H_{c,f,h,j,k}$), 7.05 (t, ^3J = 7.8 Hz, 2 H, H_g), 4.04 (s, 2 H, H_l), 2.32 (s, 6 H, H_b) ppm. UV/Vis (CH_3CN): λ_{max} (ε) = 244 (49200 $M^{-1}cm^{-1}$), 328 (26400), 342 (26100) nm. Fluorescence (CH_3CN): λ = 475 ($\Phi < 10^{-3}$) nm.

***N*,*N*′-Bis(2-tosylaminobenzylidene)-4,4′-oxodianiline (H_2L^b):** 4,4′-Oxodianiline (0.30 g, 1.50 mmol) was added to a chloroform solution (150 mL) of **3** (0.82 g, 3.00 mmol). This mixture was heated (70 °C) and the volume of the solution was reduced to about 30 mL over period of 6 h in a Dean–Stark trap. The resulting solution was filtered and then concentrated. The obtained powdery solid was collected by filtration, washed with diethyl ether (30 mL), and dried in vacuo. Yield: 1.02 g (95%). FAB MS: *m*/*z* = 715.1 [M^+ + H]. $C_{40}H_{34}N_4O_5S_2$: calcd. C 67.14, H 4.76, N 7.83, S 8.95; found C 66.37, H 4.80, N 7.92, S 8.63. IR (KBr): $\tilde{\nu}$ = 3439 ν_{N-H}, 1617 $\nu_{C=N}$, 1340 ν_{C-N}, 1289 ν_{asSO_2}, 1157 ν_{sSO_2} cm^{-1}. ^1H NMR (250 MHz, $[D_6]$-DMSO, 25 °C): δ = 12.62 (s, 2 H, H_a), 8.80 (s, 2 H, H_i), 7.76 (d, ^3J = 8.2 Hz, 2 H, H_e), 7.70 (d, ^3J = 8.2 Hz, 4 H, H_d), 7.44 (m, 8 H, $H_{h,f,k}$), 7.33 (d, ^3J = 8.2 Hz, 4 H, H_c), 7.20 (m, 6 H, $H_{f,j}$), 2.31(s, 6 H, H_b) ppm.

Metal Complexes: The neutral metal complexes $[Mn(L^a)]_2 \cdot CH_3CN$ (**1**), $[Fe(L^a)]_2 \cdot (CH_3CN)_2$ (**2**), $[Co(L^a)]_2 \cdot CH_3CN$ (**3**), $[Ni(L^a)]_2$ (**4**), $[Zn(L^a)]_2 \cdot CH_3CN$ (**5**), $[Cd(L^a)]_2$ (**6**) and $[Zn(L^b)]_2 \cdot (H_2O)_4$ (**7**) were obtained using an electrochemical procedure.[19] An acetonitrile solution of the corresponding ligand (H_2L^a or H_2L^b) containing tetraethylammonium perchlorate as supporting electrolyte was electrolyzed using a platinum wire as the cathode and a metal plate as the anode. The cell can be summarised as Pt(–)$|H_2L^{a,b}$ + MeCN|M(+), where M stands for the metal. The synthesis method is similar for all the metals except in the cases of manganese(II) and

iron(II) complexes. These two compounds were prepared in a closed cell under argon. The synthesis is typified by the preparation of **5**: A suspension (0.1 g, 0.14 mmol) of H_2L^a in acetonitrile (80 mL), containing 10 mg of tetraethylammonium perchlorate, was electrolysed for 1.5 h, using a zinc plate as anode, with a current of 10 mA. (***Caution:*** Although no problem was encountered in this work, all perchlorate salts are potentially explosive and should therefore be handled with the appropriate care!) Concentration of the resulting yellow solution to a third of its initial volume yielded a yellow solid that was washed with diethyl ether and dried under vacuum. All metal complexes were obtained with high purity and yield. Crystallisation from acetonitrile produced crystals of **5**. Unfortunately, all attempts to crystallise the other complexes were unsuccessful.

$[Mn(L^a)]_2\cdot CH_3CN$ (1): Yield: 0.081 g (84%). MS FAB: *m*/*z* = 1532.4 $[Mn_2(L^a)_2 + H]^+$. ESI MS: *m*/*z* = 1531.6 $[Mn_2(L^a)_2 + H]^+$. $C_{84}H_{71}Mn_2N_9O_8S_4$: calcd. C 64.1, H 4.5, N 8.0, S 8.1; found C 64.0, H 4.4, N 8.0, S 8.3. IR (KBr): $\tilde{\nu}$ = 1614 $\nu_{C=N}$, 1294 (C–N), 1260 ν_{asSO_2}, 1128 ν_{sSO_2} cm^{-1}.

$[Fe(L^a)]_2\cdot(CH_3CN)_2$ (2): Yield: 0.084 g (74%). MS FAB: *m*/*z* = 1534.1 $[Fe_2(L^a)_2 + H]^+$. ESI MS: *m*/*z* = 1533.4 $[Fe_2(L^a)_2 + H]^+$]. $C_{86}H_{74}Fe_2N_{10}O_8S_4$: calcd. C 63.9, H 4.6, N 8.7, S 7.9; found C 64.0, H 4.4, N 8.8, S 8.0. IR (KBr): $\tilde{\nu}$ = 1613 $\nu_{C=N}$, 1290 ν_{C-N}, 1261 ν_{asSO_2}, 1131 ν_{sSO_2} cm^{-1}.

$[Co(L^a)]_2\cdot CH_3CN$ (3): Yield: 0.095 g (86%). MS FAB: *m*/*z* = 1540.1 $[Co_2(L^a)_2 + H]^+$. ESI MS: *m*/*z* = 1539.2 $[Co_2(L^a)_2 + H]^+$. $C_{84}Co_2H_{71}N_9O_8S_4$: calcd. C 63.8, H 4.5, N 8.0, S 8.1; found C 64.0, H 4.4, N 8.1, S 8.1. IR (KBr): $\tilde{\nu}$ = 1596 $\nu_{C=N}$, 1294 ν_{C-N}, 1257 ν_{asSO_2}, 1138 ν_{sSO_2} cm^{-1}. UV/Vis (MeCN): λ_{max} (ε) = 244 (84800 $M^{-1}cm^{-1}$), 302 (47300), 384 (28700) nm.

$[Ni(L^a)]_2$ (4): Yield: 0.081 g (75%). MS FAB: *m*/*z* = 1539.8 $[Ni_2(L^a)_2 + H]^+$. ESI MS: *m*/*z* = 1539.2 $[Ni_2(L^a)_2 + H]^+$. $C_{82}H_{68}N_8Ni_2O_8S_4$: calcd. C 63.9, H 4.4, N 7.3, S 8.3; found C 64.1, H 4.4, N 7.4, S 8.1. IR (KBr): $\tilde{\nu}$ = 1601 $\nu_{C=N}$, 1303 ν_{C-N}, 1264 ν_{asSO_2}, 1131 ν_{sSO_2} cm^{-1}. UV/Vis (MeCN): λ_{max} (ε) = 246 (154900 $M^{-1}cm^{-1}$), 292 (63500), 388 (41400) nm.

$[Zn(L^a)]_2\cdot CH_3CN$ (5): Yield: 0.094 g (84%). MS FAB: *m*/*z* = 1553.5 $[Zn_2(L^a)_2 + H]^+$. ESI MS: *m*/*z* = 1552.9 $[Zn_2(L^a)_2 + H]^+$. $C_{84}H_{71}N_9O_8S_4Zn_2$: calcd. C 64.9, H 4.6, N 8.1, S 8.2; found C 64.8, H 4.5, N 8.1, S 8.3. IR (KBr): $\tilde{\nu}$ = 1614 $\nu_{C=N}$, 1299 ν_{C-N}, 1260 ν_{asSO_2}, 1141 ν_{sSO_2} cm^{-1}. ^1H NMR (250 MHz, $CDCl_3$, 25 °C): δ = 8.33 (s, 4 H, H_i), 7.91 (d, ^3J = 8.5 Hz, 8 H, H_d), 7.46–6.85 (m, 40 H, $H_{c,e-h,j,k}$), 3.89 (s, 4 H, H_l), 2.34 (s, 12 H, H_b) ppm. UV/Vis (MeCN): λ_{max} (ε) = 246 (110000 $M^{-1}cm^{-1}$), 316 (52100), 379 (40700) nm. Fluorescence (MeCN): λ = 473 (Φ = 0.03) nm.

$[Cd(L^a)]_2$ (6): Yield: 0.084 g (73%). MS FAB: *m*/*z* = 1647.7 $[Cd_2(L^a)_2 + H]^+$. ESI MS: *m*/*z* = 1646.8 $[Cd_2(L^a)_2 + H]^+$. $C_{82}H_{68}Cd_2N_8O_8S_4$: calcd. C 59.7, H 4.1, N 6.8, S 7.8; found C 59.8, H 4.0, N 6.9, S 7.9. IR (KBr): $\tilde{\nu}$ = 1603 $\nu_{C=N}$, 1289 ν_{C-N}, 1262 ν_{asSO_2}, 1127 ν_{sSO_2} cm^{-1}. ^1H NMR (250 MHz, $CDCl_3$, 25 °C): δ = 8.33 (s, 4 H, H_i), 7.93 (d, ^3J = 8.5 Hz, 8 H, H_d), 7.75 (d, ^3J = 8.5 Hz, 8 H, H_c), 7.68 (d, ^3J = 8.3 Hz, 4 H, H_e), 7.39–6.83 (m, 28 H, $H_{f-h,j,k}$), 3.95 (s, 4 H, H_l), 2.34 (s, 12 H, H_b) ppm. UV/Vis (MeCN): λ_{max} (ε) = 243 (74700 $M^{-1}cm^{-1}$), 318 (32500), 371 (27600) nm. Fluorescence (MeCN): λ = 476 (Φ = 0.01) nm.

$[Zn(L^b)]_2\cdot(H_2O)_4$ (7): Yield: 0.091 (80%). MS FAB: *m*/*z* = 1557.7 $[Zn_2(L^b)_2 + H]^+$. ESI MS: *m*/*z* = 1557.0 $[Zn_2(L^b)_2 + H]^+$. $C_{80}H_{72}N_8O_{14}S_4Zn_2$: calcd. C 58.95, H 4.42, N 6.88, S 7.86; found C 60.11, H 4.04, N 7.08, S 7.74. IR (KBr): $\tilde{\nu}$ = 1610 $\nu_{C=N}$, 1300 ν_{C-N}, 1243 ν_{asSO_2}, 1140 ν_{sSO_2} cm^{-1}. ^1H NMR (250 MHz, [D_6]-DMSO, 25 °C): δ = 8.66 (s, 4 H, H_i), 7.87 (d, ^3J = 8.2 Hz, 8 H, H_d), 7.73 (d, ^3J = 8.2 Hz, 4 H, H_e), 7.40 (m, 8 H, $H_{f,h}$), 7.29 (d, ^3J = 8.2 Hz, 8 H, H_c), 7.16 (d, ^3J = 8.2 Hz, 8 H, H_k), 6.99 (dd, ^3J = 8.2, ^3J = 6.4 Hz, 4 H, H_g), 6.87 (d, ^3J = 8.2 Hz, 8 H, H_j), 2.34 (s, 12 H, H_b) ppm.

Crystallographic Measurements: The structure determinations of **5** and $[Zn(L^b)]_2\cdot CH_3CN$ were performed at room temperature with a Siemens CCD diffractometer, using graphite-monochromated Mo-K_α radiation from a fine focus sealed tube source. Intensities were corrected for absorption (SADABS). The structures were successfully solved by direct methods (SIR97),[38b] which gave the positions of most of the non-hydrogen atoms. Remaining atoms were identified by successive Fourier difference syntheses. Refinements were carried out on F^2 by full-matrix least-square techniques using SHELXL-97.[38a] Hydrogen atoms were added in calculated positions assuming idealised bond geometries.

Acknowledgments

M. V. and M. L. thank the EU network "Molecular Level Devices and Machines" for financial support. L. S. and C. S. thank the EU network Molnanomag, MIUR and CNR for financial support. M. R. B. thanks Xunta de Galicia (PGIDIT03PXIB20901PR and PGIDIT04PXIC20902PN) and Ministerio de Educación y Ciencia of Spain (BQU2003-00167) for financial support.

[1] a) J.-M. Lehn, *Supramolecular Chemistry – Concepts and Perspectives*, VCH, Weinheim, **1995**; b) E. C. Constable, in *Comprehensive Supramolecular Chemistry* (Eds.: J. L. Atwood, J. E. D. Davies, J.-M. Lehn, D. D. MacNicol, F. Vögtle), Pergamon, Oxford **1996**, vol. 9, p. 213; c) C. Piguet, G. Bernardinelli, G. Hopfgartner, *Chem. Rev.* **1997**, *97*, 2005; d) M. Albrecht, *Chem. Rev.* **2001**, *101*, 3457; e) R. M. Yeh, A. V. Davis, K. N. Raymond, in *Comprehensive Coordination Chemistry II* (Eds.: J. A. McCleverty, T. J. Meyer), Elsevier Ltd., Oxford, **2004**, vol. 7, p. 327; f) M. J. Hannon, L. J. Childs, *Supramol. Chem.* **2004**, *16*, 7.

[2] a) M. Elhabiri, R. Scopelliti, J.-C. Buenzli, C. Piguet, *J. Am. Chem. Soc.* **1999**, *121*, 10747; b) M. J. Hannon, V. Moreno, M. J. Prieto, E. Moldrheim, E. Sletten, I. Meistermann, C. J. Isaac, K. J. Sanders, A. Rodger, *Angew. Chem. Int. Ed.* **2001**, *40*, 880; c) D. Kalny, M. Elhabiri, T. Moav, A. Vaskevich, I. Rubinstein, A. Shanzer, A.-M. Albrecht-Gary, *Chem. Commun.* **2002**, 1426; d) V. Amendola, L. Fabbrizzi, P. Pallavicini, E. Sartirana, A. Taglietti, *Inorg. Chem.* **2003**, *42*, 1632; e) C. J. Matthews, S. T. Onions, G. Morata, L. J. Davis, S. L. Heath, D. J. Price, *Angew. Chem. Int. Ed.* **2003**, *42*, 3166.

[3] a) G. Ercolani, *J. Am. Chem. Soc.* **2003**, *125*, 1609; b) M. R. Bermejo, R. Pedrido, A. M. González-Noya, M. J. Romero, M. Vázquez, L. Sorace, *New J. Chem.* **2003**, *27*, 1753; c) B. Conerney, P. Jensen, P. E. Kruger, C. MacGloinn, *Chem. Commun.* **2003**, 1274; d) S. Mizukami, H. Houjou, M. Kanesato, K. Hiratani, *Chem. Eur. J.* **2003**, *9*, 1521; e) S. D. Reid, A. J. Blake, W. Köckenberger, C. Wilson, J. B. Love, *Dalton Trans.* **2003**, 4387; f) V. Amendola, Y. Díaz Fernández, C. Mangano, M. Montalti, P. Pallavicini, L. Prodi, N. Zaccheroni, M. Zema, *Dalton Trans.* **2003**, 4340; g) R. Prabaharan, N. C. Fletcher, *Dalton Trans.* **2003**, 2558; h) K. Zeckert, J. Hamacek, J.-P. Rivera, S. Floquet, A. Pinto, M. Borkovec, C. Piguet, *J. Am. Chem. Soc.* **2004**, *126*, 11589; i) M. Elhabiri, J. Hamacek, J.-C. G. Bünzli, A.-M. Albrecht-Gary, *Eur. J. Inorg. Chem.* **2004**, 51; V. Maurizot, G. Linti, I. Huc, *Chem. Commun.* **2004**, 924; j) L. P. Harding, J. C. Jeffery, T. Riis-Johannessen, C. R. Rice, Z. Zeng, *Chem. Commun.* **2004**, 654; k) B. Quinodoz, G. Labat, H. Stoeckli-Evans, A. von Zelewsky, *Inorg. Chem.* **2004**, *43*, 7994; l) F. Tuna, M. R. Lees, G. J. Clarkson, M. J. Hannon, *Chem. Eur. J.* **2004**, *10*, 5737; m) H. Houjou, N. Schneider, Y. Nagawa, M. Kanesato, R. Ruppert, K. Hiratani, *Eur. J. Inorg.*

Chem. **2004**, 4216; n) R. Pedrido, M. R. Bermejo, M. J. Romero, M. Vázquez, A. M. González-Noya, M. Maneiro, M. J. Rodríguez, M. I. Fernández, *Dalton Trans.* **2005**, 572; o) M. Albrecht, I. Janser, R. Fröhlich, *Chem. Commun.* **2005**, 157; p) N. W. Alcock, G. Clarkson, P. B. Glover, G. A. Lawrance, P. Moore, M. Napitupulu, *Dalton Trans.* **2005**, 518.

[4] a) V. Berl, I. Huc, R. G. Khoury, J.-M. Lehn, *Chem. Eur. J.* **2001**, *7*, 2810; b) A. Lavalette, F. Tuna, G. Clarkson, N. W. Alcock, M. J. Hannon, *Chem. Commun.* **2003**, 2666; c) S. G. Telfer, R. Kurod, *Chem. Eur. J.* **2005**, *11*, 57.

[5] a) M. J. Hannon, C. L. Painting, N. W. Alcock, *Chem. Commun.* **1999**, 2023; b) S. Mizukami, H. Houjou, K. Sugaya, E. Koyama, H. Tokuhisa, T. Sasaki, M. Kanesato, *Chem. Mater.* **2005**, *17*, 50.

[6] a) C. A. Hunter, J. K. M. Sanders, *J. Am. Chem. Soc.* **1990**, *112*, 5525; b) G. R. Desiraju, T. Steiner, *The Weak Hydrogen Bond in Structural Chemistry and Biology*, Oxford University Press, Oxford, UK, **1999**; c) W. B. Jennings, B. M. Farrell, J. F. Malone, *Acc. Chem. Res.* **2001**, *34*, 885; d) R. G. Hicks, M. T. Lemaire, L. Öhrström, J. F. Richardson, L. K. Thompson, Z. Xu, *J. Am. Chem. Soc.* **2001**, *123*, 7154.

[7] a) G. R. Desiraju, A. Gavezzotti, *J. Chem. Soc., Chem. Commun.* **1989**, 621; b) W. L. Jorgensen, D. L. Severance, *J. Am. Chem. Soc.* **1990**, *112*, 4768; c) P. M. Zorky, O. N. Zrukya, *Adv. Mol. Struct. Res.* **1993**, *3*, 147; d) K. Biradha, M. J. Zaworotko, *J. Am. Chem. Soc.* **1998**, *120*, 6431.

[8] a) D. B. Amabilino, J. F. Stoddart, *Chem. Rev.* **1995**, *95*, 2725; b) K. Biradha, C. Seward, M. J. Zaworotko, *Angew. Chem. Int. Ed.* **1999**, *38*, 492; c) M. Munakata, L. P. Wu, T. Kuroda-Sowa, *Adv. Inorg. Chem.* **1999**, *46*, 173; d) M. J. Zaworotko, *Chem. Commun.* **2001**, 1.

[9] a) W. Saengew, *Principles of Nucleic Acid Structures*, Springer-Verlag, New York, **1984**, pp 132–140; b) M. R. Arkin, E. D. A. Stemp, R. E. Holmlin, J. K. Barton, A. Hormann, E. J. C. Olson, P. A. Barbara, *Science* **1996**, *273*, 475; c) S. O. Kelley, R. E. Holmlin, E. D. A. Stemp, J. K. Barton, *J. Am. Chem. Soc.* **1997**, *119*, 9861.

[10] a) P. Hobza, H. L. Selzle, E. W. Schlag, *Chem. Rev.* **1994**, *94*, 1767; b) H.-C. Weiss, D. Bläser, R. Boese, B. M. Doughan, M. M. Haley, *Chem. Commun.* **1997**, 1703; c) X.-M. Chen, G.-F. Liu, *Chem. Eur. J.* **2002**, *8*, 4811.

[11] a) S. K. Burley, G. A. Petsko, *Science* **1985**, *229*, 23; b) S. K. Burley, G. A. Petsko, *Adv. Protein Chem.* **1988**, *39*, 125.

[12] a) C. A. Hunter, *Chem. Soc. Rev.* **1994**, 101; b) M. C. T. Fyfe, J. F. Stoddart, *Acc. Chem. Res.* **1997**, *30*, 393.

[13] L. J. Childs, N. W. Alcock, M. J. Hannon, *Angew. Chem. Int. Ed.* **2002**, *41*, 4244.

[14] L. J. Childs, N. W. Alcock, M. J. Hannon, *Angew. Chem. Int. Ed.* **2001**, *40*, 1079.

[15] M. R. Bermejo, M. Vázquez, J. Sanmartín, A. García-Deibe, M. Fondo, C. Lodeiro, *New J. Chem.* **2002**, 1365.

[16] C. Janiak, *J. Chem. Soc., Dalton Trans.* **2000**, 3885.

[17] a) M. J. Hannon, C. L. Painting, N. W. Alcock, *Chem. Commun.* **1999**, 2023; b) N. Yoshida, K. Ichikawa, M. Shiro, *J. Chem. Soc., Perkin Trans. 2* **2000**, 17; c) P. E. Kruger, N. Martin, M. Nieuwenhuyzen, *J. Chem. Soc., Dalton Trans.* **2001**, 1966.

[18] M. Vázquez, A. Taglietti, D. Gatteschi, L. Sorace, C. Sangregorio, A. M. González, M. Maneiro, R. Pedrido, M. R. Bermejo, *Chem. Commun.* **2003**, 1840.

[19] M. Vázquez, M. R. Bermejo, J. Sanmartín, A. M. García-Deibe, C. Lodeiro, J. Mahía, *J. Chem. Soc., Dalton Trans.* **2002**, 870.

[20] W. K. Anderson, D. K. Dalvie, *J. Heterocycl. Chem.* **1993**, *30*, 1533.

[21] J. Mahía, M. Maestro, M. Vázquez, M. R. Bermejo, A. M. González, M. Maneiro, *Acta Crystallogr., Sect. C* **1999**, *55*, 2158.

[22] M. Vázquez, M. R. Bermejo, M. Fondo, A. M. González, J. Mahía, L. Sorace, D. Gatteschi, *Eur. J. Inorg. Chem.* **2001**, 1863, and references cited therein.

[23] Crystal structure analysis of **5**. X-ray diffraction data were collected from a yellow plate crystal (ca. $0.99 \times 0.25 \times 0.03$ mm) by means of a Smart CCD-1000 Bruker diffractometer using graphite-monochromated Mo-K_α radiation (λ = 0.71073 Å). Crystal data for $C_{84}H_{71}N_9O_8S_4Zn_2$: M = 1593.48, T = 293(2) K, monoclinic *I*2*a*, a = 34.066(9), b = 11.283(3), c = 40.426(10) Å, β = 94.673(5)°, V = 15486(7) Å^3, Z = 8, $\rho_{calcd.}$ = 1.367 g cm^{-3}, μ = 0.790 mm^{-1}, 9259 measured reflections, 9259 independent reflections with $I_0 > 2\sigma(I_0)$, 949 parameters refined, *GOF* = 0.973, R_1 = 0.0776 [$I_0 > 2\sigma(I_0)$], 0.2176 (for all data), wR_2 = 0.1979 [$I_0 > 2\sigma(I_0)$] and 0.2840 (for all data), largest difference peak and hole 1.394 and –0.782 e Å^{-3}. CCDC-231784 contains the supplementary crystallographic data for this paper. These data can be obtained free of charge from The Cambridge Crystallographic Data Centre via www.ccdc.cam.ac.uk/data_request/cif.

[24] M. Vázquez, M. R. Bermejo, M. Fondo, A. M. García-Deibe, A. M. González, R. Pedrido, *Eur. J. Inorg. Chem.* **2002**, 465.

[25] J. D. Watson, F. C. H. Crick, *Nature* **1953**, *171*, 737.

[26] a) M. Hong, G. Dong, D. Chun-Ying, L. Yu-Ting, M. Qing-Jin, *J. Chem. Soc., Dalton Trans.* **2002**, 3422; b) M. Hong, F. Chen-Jie, D. Chun-Ying, L. Yu-Ting, M. Qing-Jin, *Dalton Trans.* **2003**, 1229.

[27] Crystal structure analysis of $[Zn(L^b)]_2 \cdot CH_3CN$. X-ray diffraction data were collected from a yellow prismatic crystal (ca. $0.38 \times 0.37 \times 0.32$ mm) by means of a Smart CCD-1000 Bruker diffractometer using graphite-monochromated Mo-K_α radiation (λ = 0.71073 Å). Crystal data for $C_{82}H_{67}N_9O_{10}S_4Zn_2$: M = 1597.43, T = 293(2) K, orthorhombic *Fddd*, a = 17.102(2), b = 22.031(3), c = 40.644(6) Å, V = 15314(4) Å^3, Z = 8, $\rho_{calcd.}$ = 1.386 g cm^{-3}, μ = 0.801 mm^{-1}, 23525 measured reflections, 3791 independent reflections with $I_0 > 2\sigma(I_0)$, 242 parameters refined, *GOF* = 1.070, R_1 = 0.0441 [$I_0 > 2\sigma(I_0)$] and 0.0646 (for all data), wR_2 = 0.1287 [$I_0 > 2\sigma(I_0)$] and 0.1493 (for all data), largest difference peak and hole 0.948 and –0.275 e Å^{-3}. CCDC-261940 contains the supplementary crystallographic data for this paper. These data can be obtained free of charge from The Cambridge Crystallographic Data Centre via www.ccdc.cam.ac.uk/data_request/cif.

[28] O. M. Yaghi, H. Li, C. Davis, D. Richardson, T. L. Groy, *Acc. Chem. Res.* **1998**, *31*, 474.

[29] K. Biradha, H. Hongo, M. Fujita, *Angew. Chem. Int. Ed.* **2000**, *39*, 3843.

[30] J. Kim, B. Chen, T. M. Reineke, H. Li, M. Eddaoudi, D. B. Moler, M. O'Keeffe, O. M. Yaghi, *J. Am. Chem. Soc.* **2001**, *123*, 8239.

[31] S. Lai, C. Cheng, K. Lin, *Chem. Commun.* **2001**, 1082.

[32] E. A. Boudreax, L. N. Mulay, *Theory and Application of Molecular Paramagnetism*, Wiley, New York, **1976**.

[33] a) R. Krämer, I. O. Fritsky, H. Pritzkow, L. A. Kovbasyuk, *J. Chem. Soc., Dalton Trans.* **2002**, 1307; b) C. J. Matthews, S. T. Onions, G. Morata, L. J. Davis, S. L. Heath, D. J. Price, *Angew. Chem. Int. Ed.* **2003**, *42*, 3166 and references cited therein.

[34] E. Gottlieb, V. Kotlyar, A. Nudelman, *J. Org. Chem.* **1997**, *62*, 7512.

[35] C. J. O'Connor, *Prog. Inorg. Chem.* **1982**, *29*, 203.

[36] J. N. Demas, G. A. Crosby, *J. Phys. Chem.* **1971**, *75*, 991.

[37] Y.-H. Li, L.-M. Chan, L. Tyler, R. T. Moody, C. M. Himel, D. M. Hercules, *J. Am. Chem. Soc.* **1975**, *97*, 3118.

[38] a) G. M. Sheldrick, *SHELX-97 (SHELXS-97 and SHELXL-97), Programs for Crystal Structure Analyses*, University of Göttingen, Germany, **1998**; b) A. Altomare, M. C. Burla, M. Camalli, G. L. Cascarano, C. Giacovazzo, A. Guagliardi, A. G. G. Moliterni, G. Polidori, R. Spagna, *J. Appl. Crystallogr.* **1999**, *32*, 115.

Received: February 17, 2005
Published Online: August 2, 2005

